



THE UNIVERSITY *of* EDINBURGH

Edinburgh Research Explorer

Bacterial adhesion onto nanofiltration and reverse osmosis membranes: Effect of permeate flux

Citation for published version:

Semião, AJC, Habimana, O & Casey, E 2014, 'Bacterial adhesion onto nanofiltration and reverse osmosis membranes: Effect of permeate flux', *Water Research*, vol. 63, pp. 296–305.
<https://doi.org/10.1016/j.watres.2014.06.031>

Digital Object Identifier (DOI):

[10.1016/j.watres.2014.06.031](https://doi.org/10.1016/j.watres.2014.06.031)

Link:

[Link to publication record in Edinburgh Research Explorer](#)

Document Version:

Early version, also known as pre-print

Published In:

Water Research

General rights

Copyright for the publications made accessible via the Edinburgh Research Explorer is retained by the author(s) and / or other copyright owners and it is a condition of accessing these publications that users recognise and abide by the legal requirements associated with these rights.

Take down policy

The University of Edinburgh has made every reasonable effort to ensure that Edinburgh Research Explorer content complies with UK legislation. If you believe that the public display of this file breaches copyright please contact openaccess@ed.ac.uk providing details, and we will remove access to the work immediately and investigate your claim.



1 Bacterial adhesion onto nanofiltration and reverse osmosis
2 membranes: effect of permeate flux

3
4
5
6 *Andrea J.C. Semião¹, Olivier Habimana², Eoin Casey^{2*}*

7
8
9 ¹School of Engineering, University of Edinburgh, UK EH9 3JL

10 ²School of Chemical and Bioprocess Engineering, University College Dublin (UCD) , IRELAND

11 *Corresponding author. Mailing address: University College Dublin, School of Chemical and
12 Bioprocess Engineering, Belfield, Dublin 4, IRELAND. Phone: +353 1 716 1877, Email:

13 eoin.casey@ucd.ie

14
15
16
17
18
19 KEYWORDS: bacterial adhesion, permeate flux, nanofiltration, reverse osmosis, biofouling

20

21 **Abstract**

22 The influence of permeate flux on bacterial adhesion to NF and RO membranes was
23 examined using two model *Pseudomonas* species, namely *Pseudomonas fluorescens* and
24 *Pseudomonas putida*. To better understand the initial biofouling profile during NF/RO processes,
25 deposition experiments were conducted in cross flow under permeate flux varying from 0.5 up to
26 120 L/(h.m²), using six NF and RO membranes each having different surface properties. All
27 experiments were performed at a Reynolds number of 579. Complementary adhesion experiments
28 were performed using *Pseudomonas* cells grown to early-, mid- and late-exponential growth phases
29 to evaluate the effect of bacterial cell surface properties during cell adhesion under permeate flux
30 conditions. Results from this study show that initial bacterial adhesion is strongly dependent on the
31 permeate flux conditions, where increased adhesion was obtained with increased permeate flux,
32 until a maximum of 40% coverage was reached. Membrane surface properties or bacterial growth
33 stages was further found to have little impact on bacterial adhesion to NF and RO membrane
34 surfaces under the conditions tested. These results emphasise the importance of conducting
35 adhesion and biofouling experiments under realistic permeate flux conditions, and raises questions
36 about the efficacy of the methods for the evaluation of antifouling membranes in which bacterial
37 adhesion is commonly assessed under zero-flux or low flux conditions, unrepresentative of full-scale
38 NF/RO processes.

39

40

41 **1. Introduction**

42

43 Nanofiltration (NF) and Reverse Osmosis (RO) are well-established processes for the
44 production of high quality water. NF is principally used for the removal of hardness, trace
45 contaminants, such as pesticides and organic matter (Cyna et al. 2002), while RO is used for
46 desalination (Greenlee et al. 2009). NF and RO performance are however adversely affected by
47 biofilm formation resulting in permeate flux and quality decline (Flemming 1997, Ivnitsky et al. 2007,
48 Houari et al. 2009, Vrouwenvelder et al. 1998, Vrouwenvelder et al. 2008, Khan et al. 2013),
49 generally caused by the initial adhesion and subsequent colonization of bacterial cells on the surface
50 of the membrane, amalgamating in a biomass consisting of, and not limited to, polysaccharides,
51 proteins, and extracellular DNA (Pamp et al. 2007).

52 The first stage of biofilm formation is initiated by the adhesion of bacteria to the membrane
53 surface, a precursor of biofilm formation (Costerton et al. 1995). Previous studies have shown that
54 NF and RO membrane properties (Lee et al. 2010, Myint et al. 2010, Bernstein et al. 2011), bacterial
55 properties (Bayoudh et al. 2006, Bakker et al. 2004, Mukherjee et al. 2012) and environmental
56 conditions affect bacterial adhesion (Sadr Ghayeni et al. 1998). However, most of these studies were
57 conducted without permeate flux, which is an inherent part of NF and RO processes. The
58 hydrodynamic and concentration polarisation effects associated with flux may alter the micro-
59 environmental conditions at the interface thereby playing an important role in the characteristics
60 and rate of bacterial adhesion. A recent study showed that under the same flux conditions, the
61 biofilm formed on the surface of three different RO membranes had similar characteristics and
62 affected the membrane performance to the same extent (Baek et al. 2011): the percentage flux
63 decline was identical for all the membranes studied. In a previous study (Suwarno et al. 2012) it was
64 shown that higher permeate flux resulted in increased biovolume on the membrane surface.
65 Although previous studies suggest biofilm formation is independent of membrane surface properties

66 but dependent on pressure, no systematic studies to date have attempted to investigate the
67 relationship between initial adhesion and membrane properties at different flux conditions.

68 Surprisingly, few studies have focused on bacterial deposition under permeate flux
69 conditions (Kang et al. 2006, Kang et al. 2004, Subramani and Hoek 2008, Subramani et al. 2009,
70 Eshed et al. 2008). These studies focussed on developing an understanding of the fundamental
71 mechanisms of bacterial attachment under permeate flux conditions, often combined with the DLVO
72 theory (Derjaguin-Landau-Verwey-Overbeek theory), which describes the interactions between a
73 bacterial cell and the membrane surface taking into account Lifshitz–van der Waals (LW) and
74 electrostatic double layer (EL) interactions combined with interfacial hydrodynamic forces of cross-
75 flow lift (CL), permeation drag (PD), and gravity (G). The XDLVO theory (Extended Derjaguin-Landau-
76 Verwey-Overbeek theory) also takes into account Lewis acid–base (AB) interactions between the
77 bacterial cell and the membrane surface. Cross-flow lift (CL), permeation drag (PD), and gravity (G)
78 forces dominate bacterial movement. If the drag due to the permeating liquid is strong enough to
79 counteract the lifting force associated with cross-flow, the bacteria will be drawn towards the
80 membrane surface where it will be subjected to short range forces such as Lifshitz-van der Waal’s,
81 electrostatic double layer (EL) and Lewis acid-base interactions (AB).

82 The only studies where bacterial deposition specifically to NF and RO membranes under
83 permeate flux conditions were reported, are those from Subramani *et al.* (Subramani and Hoek
84 2008, Subramani et al. 2009) where it was found that bacterial adhesion was influenced by
85 membrane properties. However, these studies were conducted at comparatively low fluxes, of less
86 than 20 L/(h.m²) (equivalent to 2.5 bar). In full-scale NF and RO processes for water, seawater and
87 brackish water, treatment fluxes can reach up to 70 L/(h.m²) (Cyna et al. 2002, Greenlee et al. 2009,
88 Houari et al. 2009, Ventresque et al. 2000). One of the conclusions of the previous study (Subramani
89 and Hoek 2008) was that adhesion increases with permeate flux and according to the XDLVO theory,
90 permeation drag overwhelms interfacial forces at fluxes greater than 20 L/(h.m²) for Reynolds

91 numbers $Re < 200$. Furthermore, the study also concluded that the higher the Reynolds number, the
92 lower the level of concentration polarisation will be encountered for NF and RO membranes,
93 translating into increased electrostatic double layer repulsion between the negatively charged
94 bacteria and the negatively charged membrane, hence reducing adhesion rates. A high cross-flow
95 velocity is also expected to decrease adhesion due to enhanced cross-flow lift. In fact Wang et al.
96 (Wang et al. 2005) showed that increasing cross-flow velocity after adhesion experiments could
97 cause adhered bacteria to detach: this was particularly effective for adhesion permeate fluxes below
98 a “critical flux” whereby DLVO repulsion was in excess of permeation drag and bacteria adhered
99 reversibly.

100 A higher Reynolds number combined with a higher permeate flux have therefore opposing
101 effects, and it is unclear how adhesion would be influenced by permeate fluxes and Reynolds
102 numbers used in full scale NF and RO applications. To our knowledge, there are no reports in the
103 literature concerning bacterial adhesion at fluxes greater than $20 \text{ L}/(\text{h}\cdot\text{m}^2)$ for NF/RO membranes or
104 at Reynolds numbers representative of spiral wound elements in full-scale plants where values range
105 between 150 and 2000 (Schock and Miquel 1987).

106 For the broader range of membrane processes, conflicting results can be found in the literature.
107 One study showed adhesion rates onto MF membranes subjected to permeate fluxes $\sim 70 \text{ L}/(\text{h}\cdot\text{m}^2)$ to
108 be considerably different between membranes with different surface properties (Kang et al. 2006).
109 In contrast, another study (Subramani and Hoek 2008) observed a decrease in the differences of
110 adhesion rates as one increased the permeate flux through several NF and RO membranes from no
111 permeate flux up to $\sim 20 \text{ L}/(\text{h}\cdot\text{m}^2)$. A clear gap in the knowledge of bacterial adhesion to NF and RO
112 membranes was therefore identified, where the mechanisms of adhesion under common cross-flow
113 and pressure filtration conditions for different commercially available NF and RO membranes
114 needed to be clarified.

115 This paper therefore investigates the initial adhesion of two bacterial strains, *Pseudomonas*
116 *fluorescens* and *Pseudomonas putida*, to 6 different NF and RO membranes under industrially
117 relevant permeate flux conditions, as well as the adhesion of *P. fluorescens* at different growth
118 stages. *Pseudomonas*, including *Pseudomonas fluorescent* and *putida* are commonly found in NF and
119 RO biofilms during water treatment (Ivnitsky et al. 2007, Sadr Ghayeni et al. 1998, Baker and Dudley
120 1998).

121

122 **2. Materials and Methods**

123 **2.1 Model Bacteria Strains and Media**

124 The selected model bacterial strains for this study were fluorescent mCherry-expressing
125 *Pseudomonas fluorescens* PCL1701 (Lagendijk et al. 2010) and *Pseudomonas putida* PCL1480
126 (Lagendijk et al. 2010). *Pseudomonas* strains were stored at -80°C in King B broth (King et al. 1954)
127 supplemented with 20% glycerol. Cultures of both *Pseudomonas fluorescens* and *Pseudomonas*
128 *putida* were obtained by inoculating 100 mL King B broth supplemented with gentamicin at a final
129 concentration of 10 µg.mL⁻¹ using respective single colonies previously grown on King B agar (Sigma
130 Aldrich, Ireland) at 28°C. Subsequently, cultures were incubated at 28°C with shaking at 75 rpm and
131 left to grow to early exponential, mid exponential or late exponential growth stages, corresponding
132 to Optical Densities (OD₆₀₀) of 0.2, 0.6 and 1.0, respectively, for the study of the impact of bacteria
133 growth stage on adhesion to NF and RO membranes. The experiments for the study of the impact of
134 flux on the adhesion of bacteria *P. fluorescens* and *P. putida* to different NF and RO membranes
135 were performed using cells in their late exponential growth stage (OD₆₀₀=1.0).

136

137 **2.2 Microbial Adhesion to Solvents**

138 Microbial adhesion to solvents (MATS) (BellonFontaine et al. 1996) was used as a method to
139 determine the hydrophobic and Lewis acid–base surface properties of *P. fluorescens* cells at
140 different growth stages. This method is based on the comparison between microbial cell surface
141 affinity to a monopolar solvent and an apolar solvent, which both exhibit similar Lifshitz-van der
142 Waals surface tension components. Hexadecane (nonpolar solvent), chloroform (an electron
143 acceptor solvent), decane (nonpolar solvent) and ethyl acetate (an electron donor solvent) were
144 used of the highest purity grade (Sigma-Aldrich, USA). Experimentally, overnight bacterial cultures
145 grown at different stages (early, mid and late exponential phase) were washed twice in sterile 0.1 M
146 NaCl solution as described in section 2.3, and re-suspended to a final OD₄₀₀ of 0.8. Individual
147 bacterial suspensions (2.4 ml) were vortexed for 60 seconds with 0.4 ml of their respective MATS
148 solvent. The mixture was allowed to stand for 15 min to ensure complete separation of phases. One
149 mL from the aqueous phase was then removed using glass Pasteur pipettes and the final OD₄₀₀ was
150 measured. The percentage of cells residing in the solvent was calculated by the following equation:

151
152

$$\%Adherence = \frac{(OD_i - OD_f)}{OD_i} \times 100$$

153
154

155 where (OD_i) is the initial optical density of the bacterial suspension before mixing with the solvent,
156 and (OD_f) the final absorbance after mixing and phase separation. Each measurement was
157 performed in triplicate.

158

159 **2.3 Cell preparation for adhesion assay**

160 To evaluate bacterial adhesion under different flux conditions, cell concentration for each growth
161 stage (i.e. early exponential, mid exponential or late exponential growth stages) was standardized
162 by diluting the growth cultures to a final OD₆₀₀ of 0.2 in 200 mL 0.1 M NaCl (Sigma-Aldrich, Ireland).
163 This ensured a standardized starting feed cell concentration before every adhesion assay, in which

164 controlled experiments with different parameters (i.e. permeate flux and growth stage) could be
 165 compared and studied. For cells grown to early exponential phase two 100 mL cultures were
 166 prepared.

167 Cells were then harvested by centrifugation at 5000 rpm for 10 min using a Sorval RC5C Plus
 168 centrifuge (Unitech, Ireland) and a Fiberlite™ f10-6x500y fixed angle rotor (Thermo Fisher Scientific
 169 Inc., Dublin, Ireland). The supernatant was carefully discarded and the pellet re-suspended in 200 mL
 170 0.1 M NaCl solution, resulting in an inoculum consisting of approximately 10^8 cells/mL. This process
 171 was performed twice. A solution of 0.1 M NaCl was used as a model solution to mimic brackish water
 172 characteristics (Greenlee et al. 2009).

173

174 **2.4 Membranes and Cross-flow Test Unit**

175 Six NF and RO membranes were used: NF90, NF270, BW30 and BW30 FR (Dow Filmtec Corp, USA)
 176 and ESNA1-LF and ESNA1-LF2 from Hydranautics (Nitto Denko Corp, USA). BW30 FR stands for
 177 Fouling Resistant membrane. The membrane properties are presented in Table 1

178

Table 1 Membrane Properties

	Permeability (L/(h.m ² .bar)) ^a	NaCl Retention ^b (%)	Contact Angle ^c (°)	Roughness R _{MS} ^d (nm)
NF90	6.8±0.5	87.8±4.0	58.4±0.6	484.0 ± 207.1
NF270	12.6±1.2	16.0±0.3	8.4±0.5	372.9 ± 246.4
BW30	2.6±0.3	93.5±2.1	25.6±0.8	209.0 ± 41.9
BW30 FR	2.8±0.5	92.9±1.3	62.2±0.6	665.7 ± 156.9
ESNA1- LF	3.5±0.4	88.8±1.5	68.8±0.6	214.5 ± 23.4
ESNA1 – LF2	6.8±0.8	75.2±0.2	62.4±0.7	661.3 ± 97.7

179 ^a Permeability measured with MilliQ water at 21°C

180 ^b 0.1 M NaCl at 15 bar, 21°C and Re=579

181 ^c Mean contact angle of a total of 20 deionized water droplets on two independent membrane
182 samples using a goniometer (OCA 20 from Dataphysics Instruments)
183 ^d 45 μm \times 59 μm of area measured using a Wyko NT1100 optical profilometer operating in vertical
184 scanning interferometry (VSI) mode
185

186 As can be seen from Table 1 membrane surface properties varied substantially, with contact angles,
187 membrane surface roughness, and salt retention parameters ranging from 8.5° to 68.8°, 214.5 up
188 to 665.7 nm and 16.0 to 93.5%, respectively. These results clearly show the variability in surface
189 hydrophobicity as well as topographic profile of the selected membranes.

190 The cross-flow test unit used was a modified version of the unit found in a previous study (Semião et
191 al. 2013) and the schematic and operational details can be found in the Supporting Information SI.
192 Three Membrane Fouling Simulator (MFS) devices of internal channel dimensions of 0.8 mm in
193 height, 40 mm width and 255 mm length were used in parallel. No feed spacers were used in this
194 study.

195

196 **2.5 Cleaning Protocol**

197 The protocol used to clean the cross-flow system consisted of two antibacterial treatments involving
198 30 min recirculation steps of 70% Industrial Methylated Spirit (IMS, Lennox, Dublin, Ireland),
199 followed by 0.1 M NaOH. The system was rinsed in between treatments with 18.2 $\text{m}\Omega\cdot\text{cm}^{-1}$ grade 1
200 pure water (Elgastat B124, Veolia, Ireland). Since pure water is ineffective in completely removing
201 NaOH, an added step of recirculating pure water with a pH adjusted to 7 using 5 M HCl and a buffer
202 solution of 10 mM NaHCO_3 was adopted. The pH of the recirculating solution was systematically
203 checked to ensure there was no vestige of NaOH in the system. The system was then thoroughly
204 rinsed with pure water. No adhesion of fluorescent cells on a membrane compacted for 18 hours
205 with pure water occurred, showing the efficiency of the washing method.

206

207

208

209 **2.6 Adhesion Protocol**

210 Three different membranes were cut, thoroughly rinsed with pure water and left soaking overnight
211 in the fridge at 4°C. The membranes were then inserted in the cross-flow system and compacted for
212 a minimum of 18 hours at 21°C with pure water. The membrane pure water flux was measured at 15
213 bar and at the pressure subsequently used during the adhesion experiment. The cross-flow system
214 was operated in total recirculation mode (i.e. recirculation of the retentate and permeate), ensuring
215 the feed concentration and volume during the experimental runs were constant.

216 A 4 L volume of 0.1 M NaCl solution was then inserted in each feed tank (tank 1 and tank 2) and
217 recirculated in the system to remove any air bubbles. Then feed tank 2 was blocked with the ball
218 valve system and only feed tank 1 was used. Prior to inserting the bacterial cells in feed tank 1, the
219 cross-flow system was left to equilibrate at a constant selected pressure and cross-flow of 0.66
220 L.min⁻¹ (Re=579 or cross flow velocity of 0.35 m.s⁻¹) for 15 minutes with the 0.1 M NaCl solution in
221 tank 1. Selected experimental conditions consisted of monitoring bacterial adhesion at pressures
222 ranging from 3.1 to 15.5 bar, with corresponding membrane fluxes ranging up to 70 L/(h.m²) at a
223 constant temperature of 21°C. This range of fluxes was chosen to ensure coverage of the range used
224 in typical full-scale applications of NF and RO processes (Cyna et al. 2002, Greenlee et al. 2009,
225 Houari et al. 2009, Ventresque et al. 2000). In the specific case of the NF 270 membrane this range
226 was extended to 120 L/(h.m²) purely for scientific reasons, for example in the case where novel
227 membranes can operate at higher fluxes than the ones commonly applied in today's water
228 treatment plants. A bacterial inoculum containing approximately 10⁸ cells/mL was then added to
229 feed tank 1 and recirculated in the system for 30 minutes at the constant filtration conditions of
230 pressure and cross-flow as the ones used during equilibration. Permeate flux, feed and permeate

231 conductivity were measured for each membrane cell before (i.e. during equilibration with 0.1 M
232 NaCl) and after bacterial inoculation (i.e. during bacterial adhesion). After 30 minutes of adhesion,
233 feed tank 2 outlet with 0.1 M NaCl solution was opened and feed tank 1 outlet was closed in order
234 to rinse any non-adhered bacterial cells from the system under the filtration conditions used prior to
235 *ex-situ* analysis of the bacterial adhesion. Every experiment was repeated at least twice. The effect
236 of rinsing and the effect of opening the MFS for *ex-situ* analysis of bacterial surface coverage was
237 investigated by comparison with a control study performed with an MFS fitted with a sapphire glass
238 window for *in-situ* measurements. The results of these control studies are described in the
239 Supplemental Information (S2).

240

241 **2.7 Adhesion quantification**

242 Membrane Fouling Simulator (MFS) cells were separated from the system at the end of adhesion
243 experiments, and carefully opened whilst submerged in 0.1 M NaCl solution. The fouled membranes
244 were removed, 3 pieces cut from different locations of the membrane and each sample was placed
245 at the bottom of small petri dishes submerged with 0.1 M NaCl solution. The submerged fouled
246 membranes were then observed under an epi-fluorescence microscope (Olympus BX51) using a 10X
247 objective. Fluorescent mCherry-tagged *Pseudomonas* cells were observed using a 550 nm filter cube.
248 Ten micrographs were obtained at random points from each membrane sample. Cell surface
249 coverage (%) was then determined for each membrane using ImageJ[®] software, a Java-based image
250 processing program (<http://rsbweb.nih.gov/ij/>). The emission intensity of the mCherry tagged
251 *Pseudomonas cells* was found to be perfectly distinguishable from the autofluorescent background
252 of the tested membranes. In some instances, the mCherry to background fluorescence signal was
253 further improved by controlling the level of excitation light through samples using fluorescence
254 excitation balancers, attached in parallel to the light path, and by adjusting the field iris diaphragm
255 (Supporting information: S4). Acquired images were subsequently grayscaled and thresholded.

256 Bacterial deposition on membranes was then estimated as the percentage of solid surface covered
257 by bacteria, based on the number of black and white pixels of thresholded images.

258

259 **3. Results and Discussion**

260 **3.1 Effect of flux on *Pseudomonas fluorescens* adhesion**

261 The effect of permeate flux on the initial adhesion of *P. fluorescens* for different NF and RO
262 membranes is presented in Figure 1. The surface coverage of all 6 membranes was found to increase
263 from $1.6 \pm 0.2\%$ for a permeate flux of $0.5 \pm 0.1 \text{ L}/(\text{h} \cdot \text{m}^2)$ ($0.14 \mu\text{m} \cdot \text{s}^{-1}$) for the BW30 FR up to $39.4 \pm 3.3\%$
264 for a permeate flux of $35.47 \pm 0.01 \text{ L}/(\text{h} \cdot \text{m}^2)$ ($9.9 \mu\text{m} \cdot \text{s}^{-1}$) for the ESNA 1-LF2. The range of permeate
265 fluxes was extended for the particular case of the NF270 membrane, as stated in the Materials and
266 Methods section. It was found that an increase of the permeate flux from $35.47 \text{ L}/(\text{h} \cdot \text{m}^2)$ to 116
267 $\text{L}/(\text{h} \cdot \text{m}^2)$ did not significantly increase the surface coverage which was constant at around 40%.
268 Similarly, a previous study involving yeast on microfiltration membranes also correlated increased
269 cell deposition with increased permeate flux (Kang et al. 2004). Nonetheless, this present study
270 shows that bacterial adhesion reached a maximum surface coverage of around 40% for permeate
271 fluxes higher than $36 \text{ L}/(\text{h} \cdot \text{m}^2)$ as shown for membranes NF270 and ESNA1-LF2. Ridgway et al.
272 (Ridgway et al. 1984) also observed a similar plateau of adhered bacteria to a RO membrane. The
273 authors hypothesized the adhesion plateau effect to be the direct result of a limiting number of
274 adhesion sites available, independent of the increased bacterial concentration during the course of
275 the fouling experiment. More recent studies, however, have demonstrated a blocking effect caused
276 by the presence of previously adhered particles, colloids or bacterial cells (Sjollema and Busscher
277 1990, Ko and Elimelech 2000, Busscher and van der Mei 2006, Kerchove and Elimelech 2008):
278 particles or bacteria already adhered on the membrane surface can hinder bacterial adhesion on the
279 membrane surface in nearby areas causing adhesion to eventually reach a maximum.

280 Differences between a “nearly linear” adhesion (Kang et al. 2004) with increased permeate flux and
281 an adhesion that reaches a plateau, as observed in this study, could also be explained by the
282 differences in cell feed concentration. As shown in an earlier study (Kang et al. 2004), differences in
283 cell feed concentration led to significant differences in the amount of bacteria adhered when
284 subjected to identical filtration conditions; the degree of membrane fouling on a membrane will be
285 directly proportional to the bacterial concentration used, where the lower the bacterial
286 concentration, the lower the number of adhered bacterial cells.

287 NF and RO membranes have been shown to vary substantially in their surface properties. For
288 example, surface contact angle have been previously reported to range between 38.6° and 73.2°,
289 the root mean square (RMS) roughness to range between 5.9 and 130 nm and the zeta potential
290 measurement to range between -4.0 and -19.7 mV for several commercial NF and RO membranes
291 (Norberg et al. 2007). Moreover, previous studies investigating bacterial adhesion onto NF and RO
292 membranes clearly demonstrate the role of membrane surface properties on bacterial adhesion, in
293 which attributes such as membrane hydrophobicity, surface charge and roughness have shown to
294 significantly influence bacterial adhesion (Lee et al. 2010, Myint et al. 2010, Bernstein et al. 2011,
295 Kang et al. 2006, Subramani and Hoek 2008). The quantitative differences in adhesion between the
296 studied membranes were large, with bacteria adhering to some membranes up to 21 times more
297 than others. However, as previously mentioned, these studies were carried out under the absence of
298 or under very low pressure conditions (<2.5 bar), and/or at very low Reynolds numbers ($Re < 80$). One
299 of the objectives of this study was to investigate bacterial adhesion using realistic hydrodynamic
300 conditions in order to mimic NF and RO spiral-wound modules. It was observed that NF and RO
301 membrane surface properties had a small effect on bacterial adhesion under the wide range of
302 permeate flux conditions tested. The highest significant differences were obtained in the region of
303 permeate fluxes of 20 L/(h.m²), where surface coverage varied from 17.1±2.8% for the NF270 with a
304 flux of 19.0±1.3 L/(h.m²) up to 32.5±0.7% for the ESNA1-LF with a flux of 18.8±0.1 L/(h.m²). This
305 translates to the ESNA1-LF adhering only 1.8 times more than the NF270, which comparatively to the

306 previous mentioned studies (Lee et al. 2010, Suwarno et al. 2012, Kang et al. 2004) is a small
307 difference. The small differences obtained in surface coverage for these two membranes is probably
308 due to the fact that the NF270 membrane is more hydrophilic with a contact angle of 8.4° compared
309 to the ESNA1-LF which has a more hydrophobic nature, with a contact angle of 68.8°, as can be seen
310 in Table 1. Hence the more hydrophobic membrane ESNA1-LF shows greater adhesion compared to
311 the more hydrophilic membrane NF270.

312 When comparing the other membranes for a permeate flux in the region of 20 L/(h.m²), it can be
313 seen from Figure 1 that surface coverage does not vary substantially: BW30 FR with a flux of
314 21.2±5.3 L/(h.m²) has a surface coverage of 27.6±5.9%, the BW30 with a flux of 21.3±0.3 L/(h.m²) has
315 a surface coverage of 28.5±1.3% and the ESNA1-LF2 with a flux of 18.1±3.5 L/(h.m²) has a surface
316 coverage of 29.6±0.2%. The properties of the membranes tested are however very different, as can
317 be seen in Table 1: the contact angle measurements varied from 25.6° for the BW30 to 62.4° for the
318 ESNA1-LF2 and the roughness varied from 209 nm for the BW30 to 665.7 nm for the BW30-FR.
319 Despite the significant differences of the membrane surface properties surface coverage did not vary
320 substantially for the same permeate flux conditions, showing that under pressure membrane surface
321 properties have a small effect on *P. fluorescens* adhesion (Figure S3.1 in the Supporting Information).
322 This suggests that membranes with anti-bacterial or anti-biofouling properties should be tested
323 under representative pressures in order to fully assess their true performance. In contrast, adhesion
324 rates onto microfiltration membranes subjected to a permeate flux similar to the ones tested in the
325 present paper (20 μm.s⁻¹) were considerably different depending on the membrane surface
326 properties (Kang et al. 2006). These differences might be due to the tested species characteristics, to
327 different filtration conditions, different membrane surface properties such as the presence of pores
328 or to solution characteristics.

329 It was further noticed that the 30 min adhesion of bacterial cells to the membrane surface did not
330 cause a decrease in the measured permeate flux as this did not vary by more than 3% compared to

331 the flux measured before the introduction of bacterial cells into the system (i.e. during equilibration
332 with 0.1 M NaCl). Despite the adhesion of bacterial cells to the membrane surface covering up to
333 40% of the surface, this did not cause enhanced concentration polarisation that has been identified
334 in previous studies in the case of cake and biofilm formation (Herzberg and Elimelech 2007, Hoek
335 and Elimelech 2003).

336 Two main conclusions can be drawn from this study at the experimental conditions studied: (1) *P.*
337 *fluorescens* adhesion is dependent on the permeate flux and does not substantially vary for different
338 membrane properties; (2) *P. fluorescens* adhesion reached a maximum of surface coverage of 40%
339 for permeate flux higher than 35.5 L/(m².h¹).

340

341 **3.2 Effect of flux on *Pseudomonas putida* adhesion**

342 *P. putida* was employed as an alternative species in a similar series of experiments to those
343 conducted with *P. fluorescens*. The results shown in Figure 2 can be seen to follow the same trend
344 as observed with *P. fluorescens* with surface coverage increasing with permeate flux. It is clear that
345 the membrane surface properties do not have a substantial impact on the rate of bacterial adhesion
346 for the conditions tested. For a flux of 13.8±0.9 L/(h.m²) NF90 has a surface coverage of 15.5±0.9%,
347 the BW30 FR with a flux of 19.6±1.7 L/(h.m²) has a surface coverage of 16.9±3.0% and the NF270
348 with a flux of 19.0±0.3 L/(h.m²) has a surface coverage of 15.0 ±1.2%. The properties of the surfaces
349 of the membranes tested are however very different with respect to contact angle and roughness, as
350 can be seen in Table 1, showing that as for *P. fluorescens*, membrane surface properties have an
351 insubstantial effect on *P. putida* adhesion under permeate flux conditions (Figure S3.2 in the
352 Supporting Information).

353 The only difference noticed between the two bacterial species tested, *P. fluorescens* and *P. putida*,
354 was in the surface coverage rate as a function of the permeate flux (Figure 2): *P. fluorescens* reaches
355 a maximum coverage of about 40% at a permeate flux between 40 and 60 L/(h.m²) whilst *P. putida*

356 reaches a surface coverage of 40% for permeate fluxes higher than 100 L/(h.m²). These differences
357 could be associated to small differences of bacteria size. The smaller bacteria *P. putida* suffers
358 permeate drag to a lesser extent than *P. fluorescens* (Subramani and Hoek 2008) and therefore
359 adheres less for similar permeate fluxes. However due to the previously described “blocking effect”
360 mechanism, surface saturation is eventually reached by both strains at ~40% surface coverage. As *P.*
361 *fluorescens* and *P. putida* do not substantially differ in cell size, the blocking effect caused by these
362 two strains would be expected to be similar, and therefore the maximum surface coverage reached
363 is also expected to be similar.

364 The study by Subramani and Hoek (Subramani and Hoek 2008) showed that during filtration at low
365 pressures, the difference in adhesion rates between species studied was significant, but as the
366 pressure increased, corresponding to fluxes up to 20 L/(h.m²), the difference in adhesion rates
367 between species diminished resulting in similar adhesion rates at higher pressures/permeate fluxes
368 regardless of species studied. Furthermore, the same study (Subramani and Hoek 2008) showed
369 that the differences in adhesion rate of *Saccharomyces cerevisiae* on different tested membranes
370 became smaller with increasing permeate flux conditions, hence showing an overwhelming effect of
371 the convective flux compared to membrane surface properties. Although this present study differs
372 from the previous studies by focusing primarily on “end-points” following 30 minutes adhesion, a
373 common conclusion can be drawn in which higher permeate flux will lead to higher bacterial surface
374 coverage but membrane and cell surface properties have very little impact on the surface coverage.
375 The design of this present study therefore allowed a comparison of multiple membranes at different
376 flux conditions in regards to bacterial adhesion, which was especially necessary when evaluating the
377 claimed anti-fouling properties of specialized commercial membranes.

378

379

380

381 3.3 Effect of bacterial growth stage deposition under flux conditions

382 During bacterial adhesion the outer cell membrane is usually the first point of contact when
383 interacting with abiotic surfaces. The bacterial outer membrane functions as a permeability barrier
384 regulating the passage of solutes between the cell and the surrounding environment, determining
385 the physicochemical properties of the cell (Caroff and Karibian 2003, Makin and Beveridge 1996,
386 Gargiulo et al. 2007). Surface macromolecules such as lipopolysacchides and surface proteins that
387 constitute the outer membrane have been shown to significantly influence the physicochemical
388 properties of bacterial cells (van Loosdrecht et al. 1987). Moreover, the composition of
389 macromolecules on the outer membrane is known to be influenced by the bacterial growth phase
390 (Hong and Brown 2006). In one recent study (Walker et al. 2005) it was shown that the adhesion
391 profile of *Escherichia coli* was dependent on its growth phase, which was determined by the charge
392 distribution resulting from electrostatic repulsion forces. Differences in biofouling of RO membranes
393 have also been shown to depend on the growth stage of the bacterial species studied (Herzberg et
394 al. 2009). Differences were caused by the bacterial cell properties such as zeta potential. It is
395 however unclear how the growth stage impacts on the initial adhesion of bacteria onto NF and RO
396 membranes at high flux conditions. Hence the initial biofouling onto different NF and RO
397 membranes was investigated in the present study at a fixed but representative pressure (11.3 bar)
398 using bacteria at different growth phases to determine whether the effect of cell surface physico-
399 chemistry was significant. The physicochemical surface properties of *P. fluorescens* cells grown at
400 different exponential growth stages based on their affinities to different polar and apolar solvents
401 were studied and are presented in Table 2. Considerable variations in the affinity of *P. fluorescens*
402 cells to apolar solvents hexadecane and decane revealed changes in surface hydrophobicities as cells
403 enter into different exponential growth stages. Affinity to hexadecane decreased from 67.2 % to
404 27.0%, as cells enter early exponential ($OD_{600}=0.2$) to late exponential ($OD_{600}=1.0$) growth stages.
405 Likewise affinities to decane decreased from 47.6% to 28.9%.

406 A high affinity to chloroform (>94%) was observed for all tested *P. fluorescens* cells, irrespective of
 407 their growth stage. The high affinity to chloroform compared to affinities to hexadecane is an
 408 indication that the tested *P. fluorescens* cells possess a dominating electron donor character.
 409 Although lower, the affinities to ethyl acetate were on average ≈50%, irrespective of *P. fluorescens*
 410 growth state. When comparing affinities to decane and ethyl acetate, *P. fluorescens* cells grown to
 411 mid exponential (OD₆₀₀=0.6) and to late exponential phases (OD₆₀₀=1.0) possess a secondary electron
 412 acceptor character, based on their higher affinity to ethyl acetate than decane. This Lewis acid
 413 surface property is negligible for *P. fluorescens* cells entering early exponential growth stage
 414 (OD₆₀₀=0.2) as seen by their similar affinities to both decane and ethyl acetate. These results clearly
 415 indicate the subtle surface physicochemical differences between *P. fluorescens* grown at different
 416 exponential stages. Surface hydrophobicity has been shown to affect cell adhesion to surfaces (Bos
 417 et al. 1999, Habimana et al. 2007, Vanloosdrecht et al. 1987).

418

419 Table 2: Mean affinities of *P. fluorescens* at different growth stages to solvents hexadecane,
 420 chloroform, decane, and ethyl acetate. Error represents standard deviation of three replicates.

421

Growth stage OD ₆₀₀	Solvents			
	Hexadecane	Chloroform	Decane	Ethyl Acetate
0.2	67.2 ± 0.6	96.0 ± 0.2	47.6 ± 0.5	44.6 ± 5.0
0.6	41.4 ± 7.4	94.4 ± 0.9	24.1 ± 2.3	53.7 ± 3.3
1	27.0 ± 1.1	94.4 ± 1.2	28.9 ± 0.8	52.8 ± 1.1

422

423

424 In the particular case of *P. fluorescens*, there is no significant effect of the growth stage on the
 425 adhesion onto different NF and RO membranes, as shown in Figure 3 (and Figure S3.2 in the
 426 Supporting Information). It seems that the convective flux towards the membrane surface
 427 overcomes the effect of the membrane surface properties, as suggested in a previous study
 428 (Subramani and Hoek 2008).

429

430

431 **4. CONCLUSION**

432

433 This study offers an increased understanding of bacterial adhesion on NF/RO membranes under
434 conditions typically found in full-scale processes. The work presented in this paper clearly shows that
435 for representative Reynolds numbers and permeate fluxes, the membrane properties and bacterial
436 growth phases do not substantially affect initial bacterial adhesion. This has very important
437 implications, particularly for studies where anti-biofouling membranes are under evaluation: the
438 true efficiency of these membranes can only be fully evaluated when tested under realistic
439 permeate flux conditions. Future work will also need to examine biological factors involved during
440 the early stage of membrane fouling such as EPS synthesis. An understanding of these factors would
441 help better devise or select optimal processing strategies for controlling the level of fouling during
442 NF/RO processes. Furthermore, membranes labelled as Fouling Resistant such as the BW30 FR have
443 been shown to have the same initial bacterial adhesion outcome as the other membranes when
444 subjected to typical flux conditions of NF and RO membranes: the surface modifications carried out
445 on this membrane were not sufficient to avoid bacterial adhesion. This poses an important question:
446 will an efficient anti-biofouling membrane ever be developed? Should future research focus on anti-
447 adhesion surfaces or should it focus on more efficient cleaning strategies?

448

449 **Acknowledgments**

450 This research was supported by the European Research Council (ERC), project 278530, funded under
451 the EU Framework Programme 7. The authors would like to thank Mr. Pat O'Halloran for his
452 invaluable technical assistance, and Mr. Liam Morris for the construction of the MFS devices. The
453 authors especially thank Dr. Ellen L. Lagendijk from the Institute of Biology Leiden, Netherlands for
454 the gift of the *Pseudomonas fluorescens* WCS365, PCL1701 and *Pseudomonas putida* PCL 1445, PCL

455 1480 strains. The authors would final like to thank Hydranautics for kindly providing samples of the
456 ESNA1-LF and ESNA1-LF 2 membranes.

457

458 **References**

459 Cyna, B., Chagneau, G., Bablon, G. and Tanghe, N. (2002) Two years of nanofiltration at the Méry-
460 sur-Oise plant, France. *Desalination* 147(1–3), 69-75.

461 Greenlee, L.F., Lawler, D.F., Freeman, B.D., Marrot, B. and Moulin, P. (2009) Reverse osmosis
462 desalination: Water sources, technology, and today's challenges. *Water Research* 43(9), 2317-2348.

463 Flemming, H.C. (1997) Reverse osmosis membrane biofouling. *Experimental Thermal and Fluid*
464 *Science* 14(4), 382-391.

465 Ivnitsky, H., Katz, I., Minz, D., Volvovic, G., Shimoni, E., Kesselman, E., Semiat, R. and Dosoretz, C.G.
466 (2007) Bacterial community composition and structure of biofilms developing on nanofiltration
467 membranes applied to wastewater treatment. *Water Research* 41(17), 3924-3935.

468 Houari, A., Seyer, D., Couquard, F., Kecili, K., Démocrate, C., Heim, V. and Martino, P.D. (2009)
469 Characterization of the biofouling and cleaning efficiency of nanofiltration membranes. *Biofouling*
470 26(1), 15-21.

471 Vrouwenvelder, H.S., van Paassen, J.A.M., Folmer, H.C., Hofman, J.A.M.H., Nederlof, M.M. and van
472 der Kooij, D. (1998) Biofouling of membranes for drinking water production. *Desalination* 118(1–3),
473 157-166.

474 Vrouwenvelder, J.S., Manolarakis, S.A., van der Hoek, J.P., van Paassen, J.A.M., van der Meer, W.G.J.,
475 van Agtmaal, J.M.C., Prummel, H.D.M., Kruithof, J.C. and van Loosdrecht, M.C.M. (2008) Quantitative
476 biofouling diagnosis in full scale nanofiltration and reverse osmosis installations. *Water Research*
477 42(19), 4856-4868.

478 Khan, M.T., Manes, C.-L.d.O., Aubry, C. and Croué, J.-P. (2013) Source water quality shaping different
479 fouling scenarios in a full-scale desalination plant at the Red Sea. *Water Research* 47(2), 558-568.

480 Pamp, S.J., Gjermansen, M. and Tolker-Nielsen, T. (2007) The biofilm matrix: a sticky framework,
481 Horizon BioScience, Wyomondham, UK.

482 Costerton, J.W., Lewandowski, Z., Caldwell, D.E., Korber, D.R. and Lappin-Scott, H.M. (1995)
483 Microbial biofilms. *Annual Reviews in Microbiology* 49(1), 711-745.

484 Lee, W., Ahn, C.H., Hong, S., Kim, S., Lee, S., Baek, Y. and Yoon, J. (2010) Evaluation of surface
485 properties of reverse osmosis membranes on the initial biofouling stages under no filtration
486 condition. *Journal of Membrane Science* 351(1–2), 112-122.

487 Myint, A.A., Lee, W., Mun, S., Ahn, C.H., Lee, S. and Yoon, J. (2010) Influence of membrane surface
488 properties on the behavior of initial bacterial adhesion and biofilm development onto nanofiltration
489 membranes. *Biofouling* 26(3), 313-321.

- 490 Bernstein, R., Belfer, S. and Freger, V. (2011) Bacterial Attachment to RO Membranes Surface-
491 Modified by Concentration-Polarization-Enhanced Graft Polymerization. *Environmental Science &*
492 *Technology* 45(14), 5973-5980.
- 493 Bayouhd, S., Othmane, A., Bettaieb, F., Bakhrouf, A., Ouada, H.B. and Ponsonnet, L. (2006)
494 Quantification of the adhesion free energy between bacteria and hydrophobic and hydrophilic
495 substrata. *Materials Science and Engineering: C* 26(2–3), 300-305.
- 496 Bakker, D.P., Postmus, B.R., Busscher, H.J. and van der Mei, H.C. (2004) Bacterial Strains Isolated
497 from Different Niches Can Exhibit Different Patterns of Adhesion to Substrata. *Applied and*
498 *Environmental Microbiology* 70(6), 3758-3760.
- 499 Mukherjee, J., Karunakaran, E. and Biggs, C.A. (2012) Using a multi-faceted approach to determine
500 the changes in bacterial cell surface properties influenced by a biofilm lifestyle. *Biofouling* 28(1), 1-
501 14.
- 502 Sadr Ghayeni, S.B., Beatson, P.J., Schneider, R.P. and Fane, A.G. (1998) Adhesion of waste water
503 bacteria to reverse osmosis membranes. *Journal of Membrane Science* 138(1), 29-42.
- 504 Baek, Y., Yu, J., Kim, S.-H., Lee, S. and Yoon, J. (2011) Effect of surface properties of reverse osmosis
505 membranes on biofouling occurrence under filtration conditions. *Journal of Membrane Science*
506 382(1–2), 91-99.
- 507 Suwarno, S.R., Chen, X., Chong, T.H., Puspitasari, V.L., McDougald, D., Cohen, Y., Rice, S.A. and Fane,
508 A.G. (2012) The impact of flux and spacers on biofilm development on reverse osmosis membranes.
509 *Journal of Membrane Science* 405–406(0), 219-232.
- 510 Kang, S., Hoek, E.M.V., Choi, H. and Shin, H. (2006) Effect of Membrane Surface Properties During
511 the Fast Evaluation of Cell Attachment. *Separation Science and Technology* 41(7), 1475-1487.
- 512 Kang, S.-T., Subramani, A., Hoek, E.M.V., Deshusses, M.A. and Matsumoto, M.R. (2004) Direct
513 observation of biofouling in cross-flow microfiltration: mechanisms of deposition and release.
514 *Journal of Membrane Science* 244(1–2), 151-165.
- 515 Subramani, A. and Hoek, E.M.V. (2008) Direct observation of initial microbial deposition onto reverse
516 osmosis and nanofiltration membranes. *Journal of Membrane Science* 319(1–2), 111-125.
- 517 Subramani, A., Huang, X. and Hoek, E.M.V. (2009) Direct observation of bacterial deposition onto
518 clean and organic-fouled polyamide membranes. *Journal of Colloid and Interface Science* 336(1), 13-
519 20.
- 520 Eshed, L., Yaron, S. and Dosoretz, C.G. (2008) Effect of Permeate Drag Force on the Development of
521 a Biofouling Layer in a Pressure-Driven Membrane Separation System. *Applied and Environmental*
522 *Microbiology* 74(23), 7338-7347.

- 523 Ventresque, C., Gisclon, V., Bablon, G. and Chagneau, G. (2000) An outstanding feat of modern
524 technology: the Mery-sur-Oise nanofiltration Treatment plant (340,000 m³/d). *Desalination* 131(1–
525 3), 1-16.
- 526 Wang, S., Guillen, G. and Hoek, E.M.V. (2005) Direct Observation of Microbial Adhesion to
527 Membranes†. *Environmental Science & Technology* 39(17), 6461-6469.
- 528 Schock, G. and Miquel, A. (1987) Mass transfer and pressure loss in spiral wound modules.
529 *Desalination* 64, 339-352.
- 530 Baker, J.S. and Dudley, L.Y. (1998) Biofouling in membrane systems — A review. *Desalination* 118(1–
531 3), 81-89.
- 532 Legendijk, E.L., Validov, S., Lamers, G.E.M., de Weert, S. and Bloemberg, G.V. (2010) Genetic tools for
533 tagging Gram-negative bacteria with mCherry for visualization in vitro and in natural habitats,
534 biofilm and pathogenicity studies. *Fems Microbiology Letters* 305(1), 81-90.
- 535 King, E.O., Ward, M.K. and Raney, D.E. (1954) Two Simple Media for the Demonstration of Pyocyanin
536 and Fluorescin. *Journal of Laboratory and Clinical Medicine* 44(2), 301-307.
- 537 BellonFontaine, M.N., Rault, J. and vanOss, C.J. (1996) Microbial adhesion to solvents: A novel
538 method to determine the electron-donor/electron-acceptor or Lewis acid-base properties of
539 microbial cells. *Colloids and Surfaces B-Biointerfaces* 7(1-2), 47-53.
- 540 Semião, A.J.C., Habimana, O., Cao, H., Heffernan, R., Safari, A. and Casey, E. (2013) The importance
541 of laboratory water quality for studying initial bacterial adhesion during NF filtration processes.
542 *Water Research* 47(8), 2909-2920.
- 543 Ridgway, H.F., Rigby, M.G. and Argo, D.G. (1984) Adhesion of a Mycobacterium sp. to cellulose
544 diacetate membranes used in reverse osmosis. *Applied and Environmental Microbiology* 47(1), 61-
545 67.
- 546 Sjollema, J. and Busscher, H.J. (1990) Deposition of polystyrene particles in a parallel plate flow cell.
547 2. Pair distribution functions between deposited particles. *Colloids and Surfaces* 47(0), 337-352.
- 548 Ko, C.-H. and Elimelech, M. (2000) The “Shadow Effect” in Colloid Transport and Deposition
549 Dynamics in Granular Porous Media: Measurements and Mechanisms. *Environmental Science &*
550 *Technology* 34(17), 3681-3689.
- 551 Busscher, H.J. and van der Mei, H.C. (2006) Microbial adhesion in flow displacement systems. *Clinical*
552 *microbiology reviews* 19(1), 127-141.
- 553 Kerchove, A.J.d. and Elimelech, M. (2008) Bacterial Swimming Motility Enhances Cell Deposition and
554 Surface Coverage. *Environmental Science & Technology* 42(12), 4371-4377.

555 Norberg, D., Hong, S., Taylor, J. and Zhao, Y. (2007) Surface characterization and performance
556 evaluation of commercial fouling resistant low-pressure RO membranes. *Desalination* 202(1–3), 45-
557 52.

558 Herzberg, M. and Elimelech, M. (2007) Biofouling of reverse osmosis membranes: Role of biofilm-
559 enhanced osmotic pressure. *Journal of Membrane Science* 295(1–2), 11-20.

560 Hoek, E.M.V. and Elimelech, M. (2003) Cake-Enhanced Concentration Polarization: A New Fouling
561 Mechanism for Salt-Rejecting Membranes. *Environmental Science & Technology* 37(24), 5581-5588.

562 Caroff, M. and Karibian, D. (2003) Structure of bacterial lipopolysaccharides. *Carbohydrate Research*
563 338(23), 2431-2447.

564 Makin, S.A. and Beveridge, T.J. (1996) The influence of A-band and B-band lipopolysaccharide on the
565 surface characteristics and adhesion of *Pseudomonas aeruginosa* to surfaces. *Microbiology-Uk* 142,
566 299-307.

567 Gargiulo, G., Bradford, S., Simunek, J., Ustohal, P., Vereecken, H. and Klumpp, E. (2007) Bacteria
568 transport and deposition under unsaturated conditions: The role of the matrix grain size and the
569 bacteria surface protein. *Journal of Contaminant Hydrology* 92(3-4), 255-273.

570 van Loosdrecht, M.C., Lyklema, J., Norde, W., Schraa, G. and Zehnder, A.J. (1987) The role of
571 bacterial cell wall hydrophobicity in adhesion. *Appl Environ Microbiol* 53(8), 1893-1897.

572 Hong, Y. and Brown, D.G. (2006) Cell surface acid-base properties of *Escherichia coli* and *Bacillus*
573 *brevis* and variation as a function of growth phase, nitrogen source and C : N ratio. *Colloids and*
574 *Surfaces B-Biointerfaces* 50(2), 112-119.

575 Walker, S.L., Hill, J.E., Redman, J.A. and Elimelech, M. (2005) Influence of growth phase on adhesion
576 kinetics of *Escherichia coli* D21g. *Applied and Environmental Microbiology* 71(6), 3093-3099.

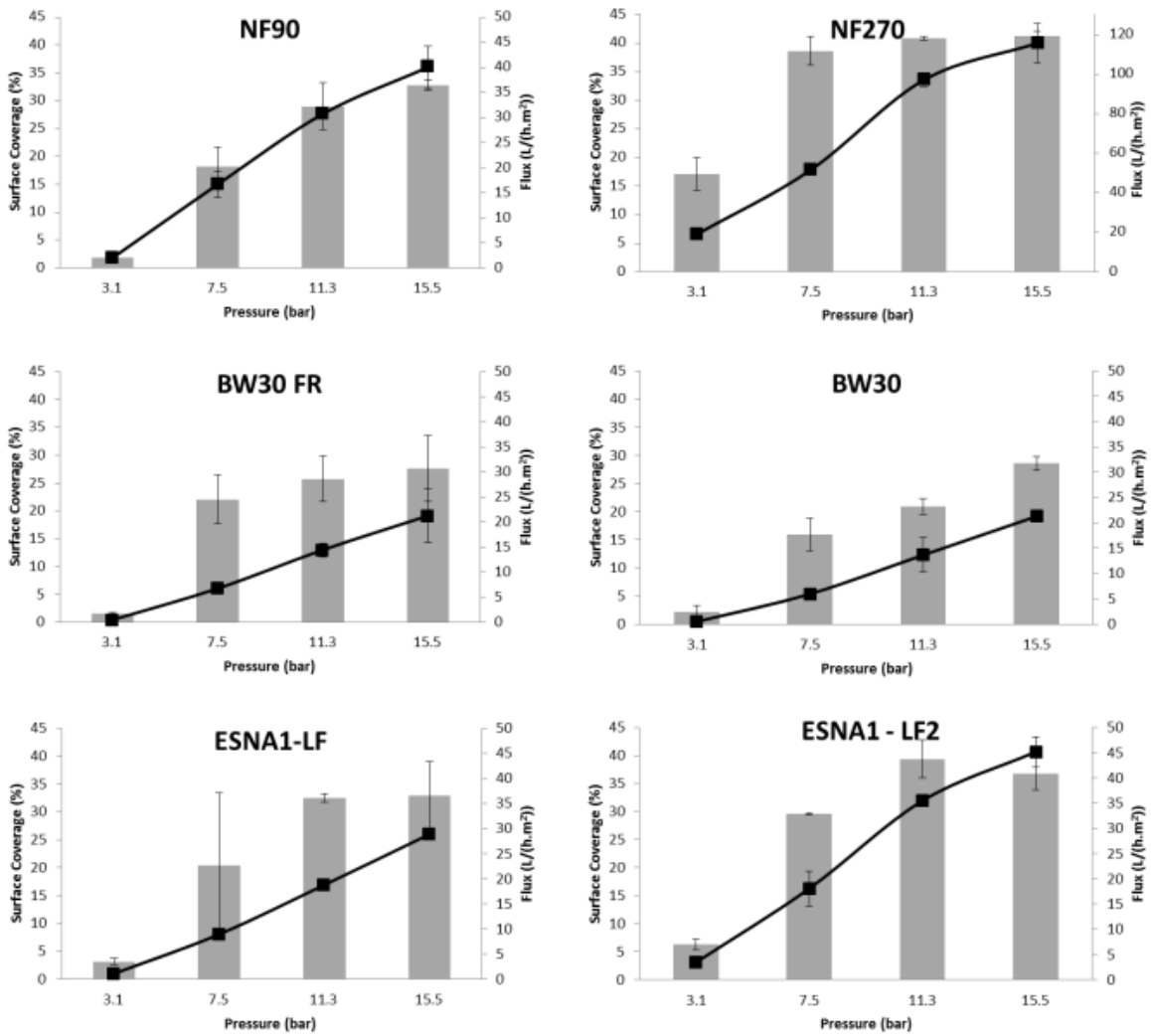
577 Herzberg, M., Rezene, T.Z., Ziemba, C., Gillor, O. and Mathee, K. (2009) Impact of Higher Alginate
578 Expression on Deposition of *Pseudomonas aeruginosa* in Radial Stagnation Point Flow and Reverse
579 Osmosis Systems. *Environmental Science & Technology* 43(19), 7376-7383.

580 Bos, R., van der Mei, H.C. and Busscher, H.J. (1999) Physico-chemistry of initial microbial adhesive
581 interactions - its mechanisms and methods for study. *Fems Microbiology Reviews* 23(2), 179-230.

582 Habimana, O., Le Goff, C., Juillard, V., Bellon-Fontaine, M.N., Buist, G., Kulakauskas, S. and Briandet,
583 R. (2007) Positive role of cell wall anchored proteinase PrtP in adhesion of lactococci. *Bmc*
584 *Microbiology* 7.

585 Vanloosdrecht, M.C.M., Lyklema, J., Norde, W., Schraa, G. and Zehnder, A.J.B. (1987) Electrophoretic
586 Mobility and Hydrophobicity as a Measure to Predict the Initial Steps of Bacterial Adhesion. *Applied*
587 *and Environmental Microbiology* 53(8), 1898-1901.

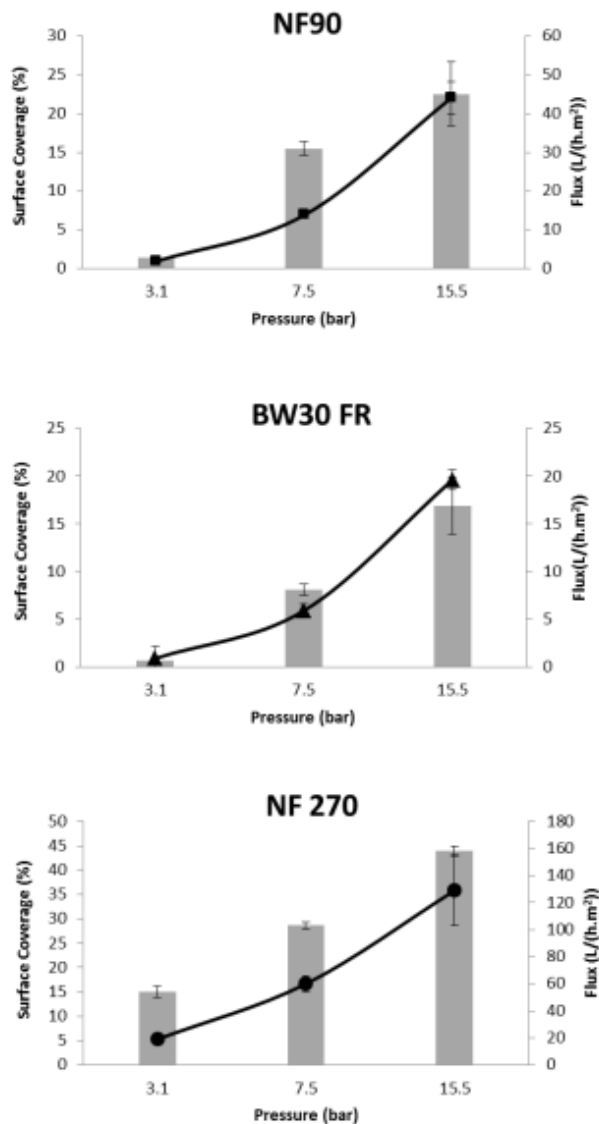
588



590

591 Figure 1: Effect of flux on *P. fluorescens* surface coverage of NF and RO membranes: columns
 592 represent surface coverage and black squares represent permeate flux (10^7 cells/mL, 0.1 M NaCl,
 593 21°C, pH~7, 0.66 L.min⁻¹ or Re=579, each experiment repeated at least twice). Error bars show
 594 standard deviation of repeated experiments.

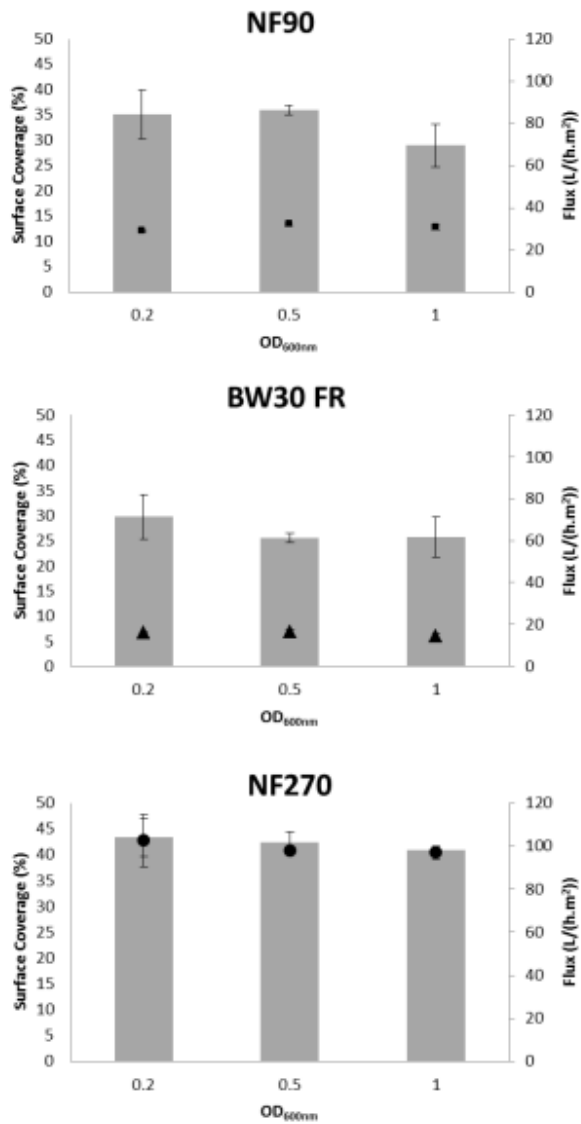
595



596

597 Figure 2: Effect of flux on *P. putida* surface coverage of NF and RO membranes: columns represent
 598 surface coverage and black squares represent permeate flux (10^7 cells/mL, 0.1 M NaCl, 21°C, pH~7,
 599 $0.66 \text{ L}\cdot\text{min}^{-1}$ or $\text{Re}=579$, each experiment repeated at least twice). Error bars show standard
 600 deviation of repeated experiments. (Note: the permeate flux is apparently not seen as a linear
 601 relationship with pressure because the columns are not equally spaced in pressure. The linear
 602 correlation coefficient of permeate flux vs pressure is in fact $r^2 > 0.995$ for these experiments).

603



604

605 Figure 3: Effect of *P. fluorescens* growth stage on surface coverage of NF and RO membranes:
 606 columns represent surface coverage and black squares represent permeate flux (10^7 cells/mL, 0.1 M
 607 NaCl, 21°C, pH~7, 0.66 L.min⁻¹ or Re=579, 11.3 bar, each experiment repeated at least twice). Error
 608 bars show standard deviation of repeated experiments.

609